Journal of Power Sources 189 (2009) 1127–1131

Contents lists available at ScienceDirect

Journal of Power Sources

journal homepage: www.elsevier.com/locate/jpowsour

Short communication

The impact of sulfur on the performance of a solid oxide fuel cell (SOFC) system operated with hydrocarboneous fuel gas

Florian P. Nagel [a], Tilman J. Schildhauer [a,*], Josef Sfeir [b], Alexander Schuler [b], Serge M.A. Biollaz [a]

[a] Paul Scherrer Institut, Laboratory for Energy and Materials Cycles, Department General Energy, CH-5232 Villigen PSI, Switzerland
[b] Hexis AG, Hegifeldstrasse 30, CH-8404 Winterthur, Switzerland

ARTICLE INFO

Article history:
Received 3 June 2008
Received in revised form 10 December 2008
Accepted 20 December 2008
Available online 30 December 2008

Keywords:
SOFC
Sulfur
Internal reforming
Open circuit voltage
Performance loss

ABSTRACT

The impact of thiophene in the fuel gas of a commercial solid oxide fuel cell (SOFC) system is investigated for concentrations up to 400 ppmV. Based on the measured voltage–current curves, an empiric correlation for the estimation of the expectable power output of the investigated SOFC system when operated with sulfur containing fuel gases is derived. An interrelation between the open circuit voltage (OCV) and the sulfur concentration of the investigated hydrocarboneous fuel gas is presented and discussed based on corresponding model simulations. The reduction of the steam reforming (STR) activity of the anode cermet material and of the catalytic partial oxidation catalyst used for the fuel gas processing in the investigated SOFC system are found important factors regarding the power output reduction induced by sulfur traces in the fuel gas of SOFCs.

1. Introduction

Power generation by means of solid oxide fuel cells (SOFC) has drawn a lot of interest in the past years. This is due to their less stringent requirements to the fuel gas quality compared to other fuel cell types and their capability of directly oxidizing hydrocarboneous fuel gases with high efficiencies at small scale. At present, the primary targeted fuel for SOFCs is natural gas, which is usually odorized by the distributors for safety reasons by addition of organic sulfur species allowing for the fast identification of leaks of natural gas appliances and pipelines. However, sulfur is a well-known poison for nickel catalysts, [1], whereby the type of sulfur specie is usually unimportant for the poisoning, [2]. Sulfur chemisorbs on nickel, thus blocking active nickel sites. The poisoning effect of sulfur on the electrochemical performance of SOFCs has been the subject of numerous studies, where it is often reported to be reversible and less pronounced at higher temperatures, [3–7]. It leads to an almost instant reduction of the steam reforming (STR) activity and to shortening of the active length of the triple phase boundary of the commonly employed nickel cermet anodes of SOFCs. Hence, activation polarization losses increase very fast when sulfur is present in the fuel gas. For instance in [7], 1 ppmV of H_2S was reported to cause an almost instant 15% performance drop. In this work, we investigate the impact of thiophene on the performance of a commercial SOFC system operated at around 950 °C with catalytically partially oxidized (CPO) methane. Thiophene was chosen as model component for the organic sulfur species usually employed as natural gas odorants because it is easy to handle and to dose. We present an empiric correlation for sulfur induced performance losses and propose three coupled mechanisms to explain the observed performance losses.

2. Experimental

The primary targeted fuel of the investigated SOFC system is odorized natural gas. The cells exhibit some tolerance towards sulfur traces in the fuel gas due to the employed anode materials and the high operating temperature of 950 °C. Fig. 1 shows the investigated SOFC system. The cell is of a planar circular design and electrolyte supported. The flow pattern of the anode and cathode gas is co-current. The investigated SOFC system comprises 63 metallic current collectors and electrode–electrolyte assemblies. The active area per cell is approx. 100 cm^2. The maximum electrical output of the system is around 1 $kW_{el,DC}$. Air is introduced to the SOFC stack via an air pre-heater. The pre-heated air enters the SOFC stack on the cathode side through four air channels which are formed by the metallic interconnector plates and the electrode–electrolyte assemblies. After participating in electrochemical reactions, Eq. (3), the depleted air exits the stack radially

Abbreviations: CPO, catalytic partial oxidation; DC, direct current; OCV, open circuit voltage; SOFC, solid oxide fuel cell; STR, steam reforming; TPB, triple phase boundary; WGS, water gas shift; YSZ, yttria stabilized zirconia.

* Corresponding author.
E-mail address: tilman.schildhauer@psi.ch (T.J. Schildhauer).

0378-7753/$ – see front matter © 2008 Elsevier B.V. All rights reserved.
doi:10.1016/j.jpowsour.2008.12.092

Nomenclature

E	voltage (V)
F	Faraday constant (C mol^{-1})
K_p	equilibrium constant
$\dot{n}$	molar flow (mol s^{-1})
p	total or partial pressure (N m^{-2})
r_j	reaction rate of reaction j (mol sec^{-1} m)
R	resistance or ideal gas constant (W) or (J mol^{-1} K)
TsK	solid structure temperature (K)
y	molar fraction (–)

Greek symbol

ν_{ij}	stoichiometric coefficient of specie i in reaction j (–)

Subscripts and superscripts

el	electric
oxi	oxidation
S	sulfur
STR	steam reforming

and takes part in the post-combustion of the partially depleted fuel.

$$H_2 + O^{2-} \leftrightarrow H_2O + 2e^- \quad (1)$$

$$CO + O^{2-} \leftrightarrow CO_2 + 2e^- \quad (2)$$

$$O_2 + 4e^- \leftrightarrow 2O^{2-} \quad (3)$$

Prior to be fed to the SOFC stack, the odorized natural gas is catalytically partially oxidized in a catalyst monolith operated with an air-to-fuel ratio of 0.27. The overall reaction is stated in Eq. (4). Two reaction zones establish in the monolith. In the first zone, the inflowing methane is predominantly oxidized at temperatures up to 1100 °C consuming all available oxygen according to Eq. (5). In the second zone, parts of the unreacted methane are steam and dry reformed, Eqs. (6) and (7), and the products are shifted, Eq. (8), using the heat and the reaction water originating from the first zone. Overall, the reactions occurring in the second zone are endothermic, resulting in a temperature of the CPO gas at the monolith exit of around 700 °C, which is suitable for the SOFC stack.

$$CH_4 + 0.5O_2 \rightarrow CO + 2H_2 \quad (4)$$

$$CH_4 + 2O_2 \rightarrow CO_2 + 2H_2O \quad (5)$$

$$CH_4 + H_2O \leftrightarrow CO + 3H_2 \quad (6)$$

$$CH_4 + CO_2 \rightarrow 2CO + 2H_2 \quad (7)$$

$$CO + H_2O \leftrightarrow CO_2 + H_2 \quad (8)$$

The CPO gas is introduced to the SOFC stack through a central fuel gas channel. The remaining methane in the CPO gas is reformed on the anode of the cells of the investigated SOFC system according to Eq. (6). Shift reactions take place on the anode as well. After partial electrochemical conversion to water and carbon dioxide, Eqs. (1) and (2), the depleted fuel gas is mixed with the depleted air and combusted. The exhausts are used for the pre-heating of the fresh air.

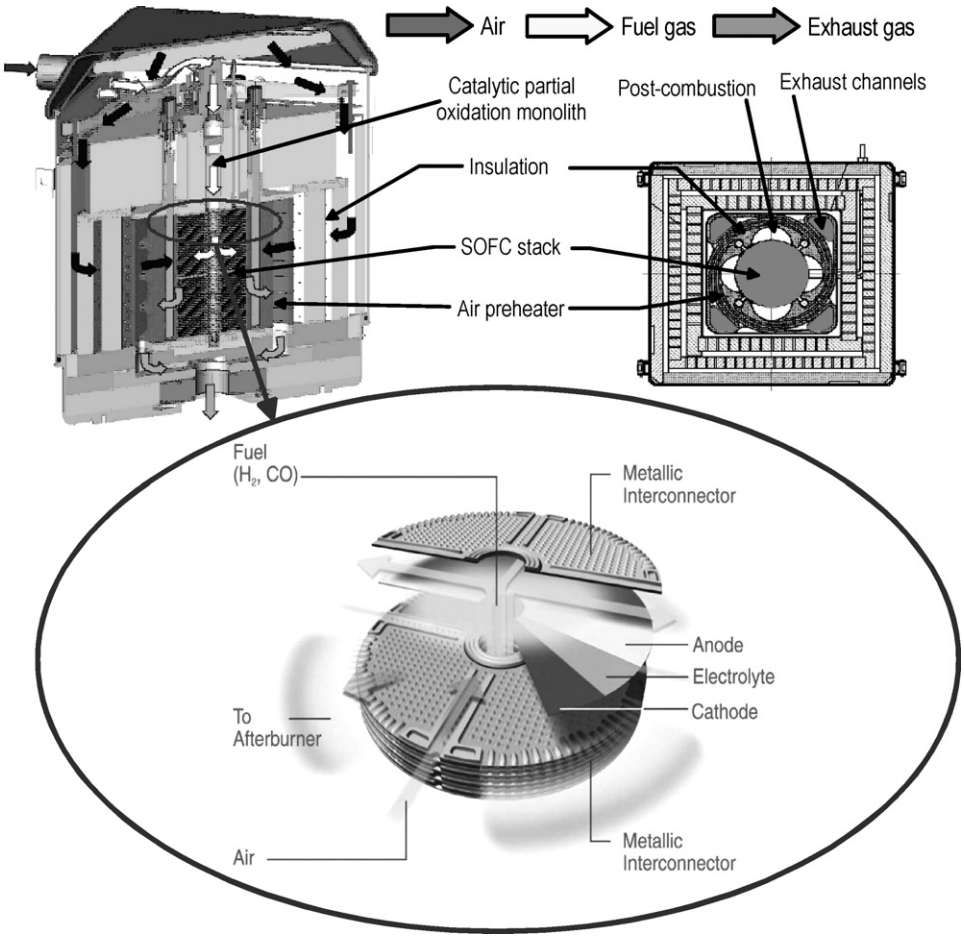

Fig. 1. The investigated SOFC system, [16].

For the presented investigation, pure methane was used as model fuel gas. Thiophene was added to the methane using a saturator installed in an ice bed. Argon was used as carrier gas. The thiophene concentration in the methane was adjusted through the carrier gas flow rate. This setup allowed producing thiophene concentrations in the methane up to 400 ppmV. This translates into approx. 80 ppmV at the cell inlet, due to the volume expansion of the fuel gas resulting from the CPO. To account for the adsorption of sulfur on the metallic surfaces, the voltage–current curves were only recorded after several hours of steady-state operation of the SOFC system with the corresponding sulfur containing fuel gas being achieved. Assuming that in steady-state the adsorption and desorption of sulfur on the metallic surfaces of the feed line occur at equal rates, the sulfur concentration at the cell inlet should correspond to the set value.

3. Model definition

The impact of the reforming activity on the open circuit voltage (OCV) was investigated with the SOFC model discussed in depth in [8]. The most important equations regarding this work are given below. The spatial distribution of the Nernst voltage, $E_{\mathrm{Nernst,H2}}$, is calculated based on the local species partial pressures using Eq. (9).

$$E_{\mathrm{Nernst,H_2}} = \left(\frac{R \times \mathrm{TsK}}{2F}\right)\left(\ln Kp_{\mathrm{H_2,oxi}} + \ln\left(\frac{p_{\mathrm{H_2}} p_{\mathrm{O_2}}^{0.5}}{p_{\mathrm{H_2O}}}\right)\right) \quad (9)$$

The values of the equilibrium constants for the hydrogen oxidation, $Kp_{\mathrm{H_2,oxi}}$, were taken from [9]. The employed model considers the water gas shift reaction (WGS) always at thermodynamic equilibrium. The reaction rates of the STR of the remaining methane in the CPO gas taking place at the anode, Eq. (6), are computed through Eq. (10), taken from [10].

$$r_{\mathrm{CH_4STR,Ach}} = 4274.0\ \mathrm{mol\,m^{-2}\,s^{-1}\,bara^{-1}}\, p_{\mathrm{CH_4}} \times \exp\left(\frac{-82,000\ \mathrm{J\,mol^{-1}}}{R \times \mathrm{TsK}}\right) \quad (10)$$

Knowing all important reaction rates, the spatial distribution of the species along the anode channel can be computed according to the differential Eq. (11).

$$\frac{d\dot{n}_i}{dx} = \sum_1^j \nu_{ij} r_j \ \text{with}\ i = \mathrm{H_2},\ \mathrm{CO},\ \text{etc. and}\ j = \mathrm{WGS},\ \mathrm{STR},\ \text{etc.} \quad (11)$$

4. Results and discussion

4.1. Measurements

Fig. 2 shows the measured voltage–current curves for varying thiophene concentrations. The investigated SOFC was soundly operable even with the highest tested sulfur concentrations. The power output, however, declined considerably with increasing sulfur concentrations. The sulfur induced power losses can be expressed with the fit correlation stated by Eq. (12) and shown in Fig. 3. $x_{\mathrm{S,loss}}$ represents the fraction of power output that the investigated SOFC system, operated at 42 V, with sulfur containing fuel gases produced in comparison to sulfur-free fuel gas. y_{S} represents the molar fraction of the total sulfur content in the fuel gas at the cell inlet in ppmV.

$$x_{\mathrm{S,loss}} = 0.52695 + 0.20716\ \exp\left(-\frac{5y_{\mathrm{S}}}{18.804}\right) + 0.26521 \times \exp\left(-\frac{5y_{\mathrm{S}}}{135.374}\right) \quad (12)$$

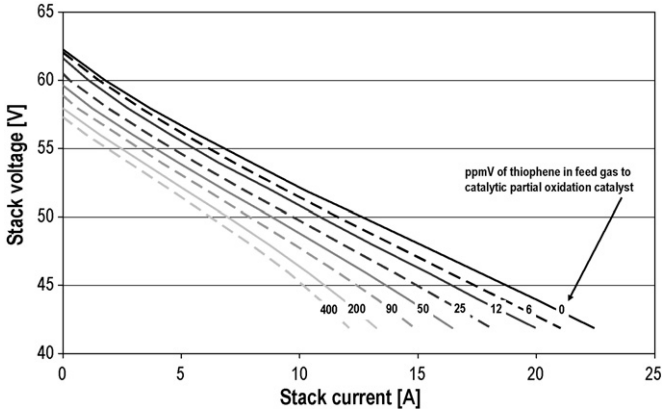

Fig. 2. Voltage–current curves obtained from the investigated SOFC stack for different sulfur concentrations.

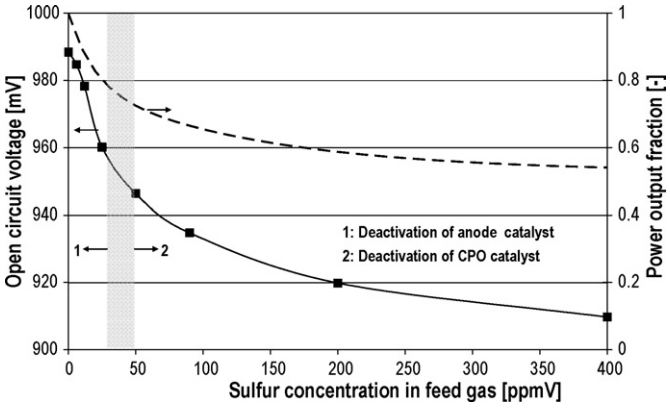

Fig. 3. Open circuit voltage and power output fraction for different sulfur concentrations.

From Fig. 2 it can be seen that the power output declined due to decreasing OCVs and steeper slopes of the voltage–current curves. The steeper slopes may be explained by limitations of the electrochemical reactions due to the blocking of active sites at the fuel electrode–electrolyte interface as reported in [3]. The decline of the OCV follows an s-shaped curve, Fig. 3. This indicates that at least two mechanisms must be active.

4.2. Model based analysis of sulfur impact on OCV

The OCV decrease between 0 and 30 ppmV could be a consequence of the deactivation of the nickel-based anode catalyst with respect to STR reactions. The deactivation of the catalyst was modeled by reducing the pre-exponential factor in Eq. (10). Similar to the experiments, methane after a CPO with an air-to-fuel ratio of 0.27 was assumed as fuel gas for the model calculations. The fuel and the air composition are given in Table 1. In OCV operation the

Table 1
CPO gas composition for 85% and 60% conversion and air composition used for the model simulations.

Specie	Unit	CPO gas at 100% catalyst activity	CPO gas at 70% catalyst activity	Air
Hydrogen	mol%	31.00	21.42	–
Carbon monoxide		14.50	9.32	–
Carbon dioxide		2.60	4.76	–
Water		3.60	6.75	–
Methane		4.40	9.61	–
Nitrogen		43.90	48.14	79.00
Oxygen		–	–	21.00

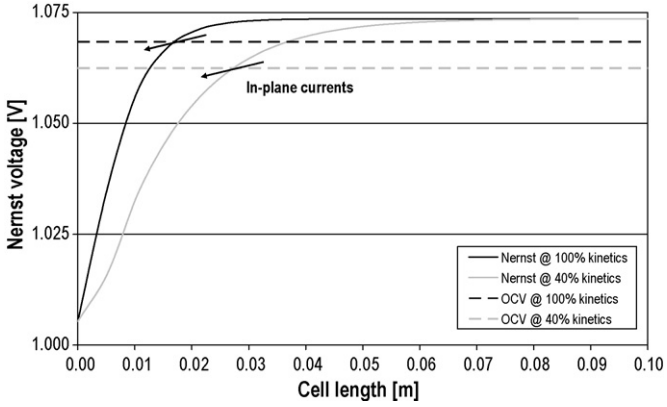

Fig. 4. Calculated Nernst voltage distributions and effective open circuit voltages for 100% and 40% reforming activity.

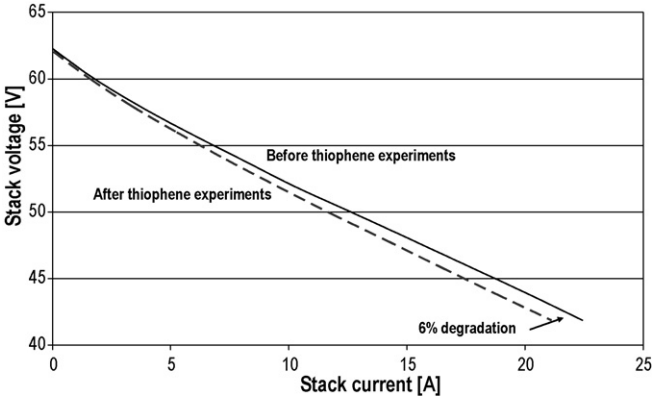

Fig. 6. Comparison of voltage–current curves obtained before and after sulfur experiments.

entire fuel is converted in the post-combustion zones which directly heat the stack. Thus, isothermal conditions were assumed with a temperature of 950 °C. The exact geometry of the investigated cell was not considered, instead the generalized planar geometry used in [8] was assumed. Despite these simplifications, the modeling results give an indication about the impact of the proposed OCV drop mechanism.

Due to the assumption that the WGS is always at equilibrium, the carbon monoxide/carbon dioxide Nernst voltage equals the hydrogen/water Nernst voltage. The following discussion therefore focuses on the hydrogen/water Nernst voltage only. Fig. 4, shows the hydrogen/water Nernst voltage distributions for a fully active anode catalyst and a catalyst with 40% of the initial STR activity.

Assuming the interconnector plates as equipotential, the effective OCV is the voltage at which the sum of in-plane currents is zero. The effective OCV drops considerably with decreasing STR activity due to flattened Nernst voltage distributions. Fig. 5 correlates the OCV drop with the STR activity. Assuming that the first 30 mV of OCV drop in Fig. 3 results from reduced STR activity leads to approx. 90% deactivation according to Fig. 5. This magnitude of deactivation is reasonable for high-temperature STR catalysts operated at 950 °C with total sulfur concentrations of 10 ppmV, [1]. However, in the experiment the total sulfur concentration at the cell inlet causing 30 mV OCV drop was about 5 ppmV. Considering that in the regions where STR reactions take place the temperatures can be up to 200 K lower than the average cell temperature, leads to critical total sulfur concentrations of 1 ppmV, [1]. Therefore, a 90% deactivation with 5 ppmV of sulfur in the fuel gas seems reasonable.

The second mechanism which could play an important role for the observed OCV drop is the deactivation of the CPO catalyst. Lower

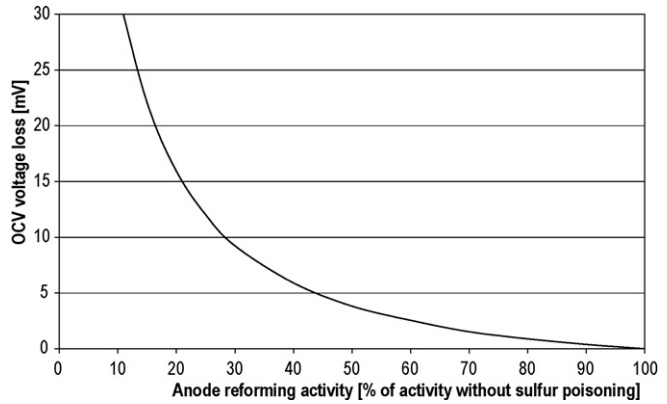

Fig. 5. Calculated OCV drop for varying reforming activities.

conversion rates of the CPO yield less hydrogen and more water. The worse hydrogen-to-water ratios directly yield lower OCV values, see Eq. (9). To account for a 50 mV of OCV drop, the activity of the CPO would have to be reduced by approx. 30% yielding the second CPO gas composition given in Table 1. The double potential formation between hydrogen/water and hydrogen sulfide/sulfur dioxide could be another explanation for the observed OCV drop, [4]. However, this mechanism was not investigated in depth yet. Future experiments will focus on hydrogen as model fuel, the Nernst voltage of which is independent of the STR activity, to prove or disprove the proposed hypotheses.

4.3. Permanent degradation of test stack

Fig. 6 compares the voltage–current curves obtained before and after the sulfur experiments. It is well known, that nickel-based catalysts operated at high-temperatures can be regenerated after sulfur poisoning by switching to a sulfur-free fuel gas, [1,11]. However, excessive sulfur concentrations can cause permanent degradation via bulk sulfidation, [12]. Besides, state-of-the-art Ni–yttria stabilized zirconia (YSZ) SOFC anodes predominantly degrade due to the agglomeration and coarsening of the nickel particles which are dissolved in an YSZ matrix. The formation of isolated large nickel islands in the YSZ matrix has two effects. First, the reduction of the specific nickel surface and of the attributed size of the triple phase boundary leads to an increase of the activation polarization, [13]. And second, the coarsening of nickel particles leads to losses of nickel particle percolation. The reduced number of direct Ni–Ni contacts results in a lower electrical conductivity of the anode and increased ohmic polarization, [14]. Thus, irreversible degradation through enhanced nickel particle sintering may be caused by sulfur as it easily reacts with nickel, forming e.g. nickel sulfide (Ni_2S_3), [15], which melts at 806 °C compared to 1455 °C of pure nickel, [15]. Both mechanisms may account for the 6% permanent degradation found after the discussed experiments.

5. Conclusions

The impact of various thiophene concentrations in the fuel gas of a commercial SOFC system was investigated. The SOFC system could be soundly operated with thiophene concentrations of up to 400 ppmV in the raw fuel gas. An empiric correlation was derived from the measured voltage–current curves for the estimation of the power output of the investigated SOFC system when operated with sulfur containing fuel gases. For the investigated hydrocarboneous fuel gas, an interrelation between the OCV and the sulfur concentration was found. Based on model simulations, the OCV decline observed for increasing sulfur concentrations was

attributed to a considerable reduction of the STR activity of the anode cermet material of the investigated SOFC, on the one hand, and to a reduction of the activity of the CPO catalyst used for the fuel gas processing in the investigated SOFC system, on the other hand. Despite the frequently reported reversible character of sulfur poisoning, permanent degradation was found.

References

[1] M.V. Twigg, Catalyst Handbook, Wolfe Publishing Ltd., Frome, England, 1989.
[2] U. Hennings, M. Brune, R. Reimert, GWF Gas Erdas 145 (2004) 92–97.
[3] Y. Matsuzaki, Y. Isamu, Solid State Ionics 132 (2000) 261–269.
[4] L. Aguilar, S. Zha, Z. Cheng, J. Winnick, M. Liu, J. Power Sources 135 (2004) 17–24.
[5] N. Arnstein, Experimental Investigation of Solid Oxide Fuel Cells Using Biomass Gasification Producer Gases, Norwegian University of Science and Technology, Trondheim, Norway, 2005.
[6] R.H. Cunningham, M.Fowles, R.M. Ormerod, J. Staniforth, Sulphur Poisoning of the Active Materials Used in SOFCs, DTI, Report F/01/00222/REP, 2004.
[7] O. Marina, L.R. Pederson, D.J. Edwards, C.W. Coyle, J. Templeton, M. Engelhard, Z. Zhu, SOFC Operation on Hydrogen and Coal Gas in the Presence of Phosphorus, Arsenic and Sulfur Impurities, in: Proceedings of the 8th Annual SECA Workshop, San Antonio, United States of America, 2007, 7–9 August.
[8] F.P. Nagel, T.J. Schildhauer, S.M.A. Biollaz, A. Wokaun, J. Power Sources 184 (2008) 143–164.
[9] E. Schmidt, Einführung in die Technische Thermodynamik, Springer, Berlin, Göttingen, Heidelberg, Germany, 1963.
[10] E. Achenbach, E. Riensche, J. Power Sources 52 (1994) 283–288.
[11] S.C. Singhal, K. Kendall, Design and Applications, Elsevier, London, Great Britain, 2004.
[12] A.L. Dicks, J. Power Sources 61 (1996) 113–124.
[13] E. Ivers-Tiffee, A. Weber, D. Herbstritt, J. Eur. Ceram. Soc. 21 (2001) 1805–1811.
[14] D. Simwonis, F. Tietz, D. Stover, Solid State Ionics 132 (2000) 241–251.
[15] R. Stübner, Untersuchungen zu den Eigenschaften der Anode der Festoxid-Brennstoffzelle SOFC, Technische Universität Dresden, Dresen, Germany, 2002.
[16] Website, www.hexis.com, January 2008.